

THE PHYSICAL REVIEW

A journal of experimental and theoretical physics established by E. L. Nichols in 1893

SECOND SERIES, VOL. 185, No. 5

25 SEPTEMBER 1969

Electron Antineutrino Interaction with Deuterons[†]

T. L. JENKINS

Department of Physics, Case Western Reserve University, Cleveland, Ohio 44106

AND

F. E. KINARD*

E. I. DuPont de Nemours and Company, Savannah River Laboratory, Aiken, South Carolina 29801

AND

F. REINES

Department of Physics, University of California, Irvine, California 92664

(Received 4 June 1969)

The reaction $d(\bar{\nu}_e, e^+)2n$ has been observed using antineutrinos from a powerful fission reactor. The measured cross section $\bar{\sigma}_{\text{expt}} = 3.0 \pm 1.5 \times 10^{-46}$ cm²/fission $\bar{\nu}_e$ is consistent with expectations, $\bar{\sigma}_{\text{theor}} = 2.4 \pm 0.4 \times 10^{-46}$ cm²/fission $\bar{\nu}_e$, based on the two-component neutrino theory and elementary considerations regarding the structure of the deuteron.

INTRODUCTION

THE interaction between $\bar{\nu}_e$ and the deuteron,

$$\bar{\nu}_e + d \rightarrow n + n + e^+, \quad (1)$$

is completely specified at low energies by the theory of weak interactions and a knowledge of the deuteron's structure. However, unlike the reaction $p(\bar{\nu}_e, e^+)n$ with its observed inverse neutron decay, the corresponding inverse reaction for $\bar{\nu}_e + d$ —i.e., $n + n \rightarrow d + e^- + \bar{\nu}_e$ —is not accessible to direct experimental check.

An additional feature of the deuteron reaction is the pure Gamow-Teller or axial-vector coupling involved as opposed to the mixture of Gamow-Teller and Fermi or vector coupling associated with neutron decay. It will be recalled that Gamow-Teller coupling is required in the present case because the final state is an *S* state and the Pauli principle requires that the product neutrons have antiparallel spins. It would be interesting to see if the expected factor-of-2 cross-section enhancement due to parity nonconservation obtains in the deuteron case as it appears to do in the proton case.¹

From a strictly experimental point of view the astrophysically important reaction $p + p \rightarrow d + e^+ + \nu_e$

has not been seen in terrestrial laboratories. An observation of the $\bar{\nu}_e + d$ reaction is, in the sense of charge independence of the weak interaction strength, equivalent to observation of this weak $p + p$ reaction.

An additional feature of the $\bar{\nu}_e + d$ reaction is the low energy which the product neutrons can have relative to each other. This fact tends to accentuate the effect of the final-state *n, n* interaction.

Unfortunately, this first experiment was not of sufficient accuracy, nor were the various particles involved observed in sufficient detail to give a better than extremely crude check on the various features mentioned. In fact, the purpose of the experiment was largely to see whether the numerous difficulties attendant on observing a reaction with such a minuscule cross section ($\sim 2 \times 10^{-46}$ cm² for fission $\bar{\nu}_e$) could be overcome. The one previous attempt made to observe this reaction only set an upper limit.² As we describe in this paper, we have observed the reaction and the way is now somewhat clearer to a more precise experiment.

The present approach again uses the copious flux of $\bar{\nu}_e$ from a powerful fission reactor (2.8×10^{13} $\bar{\nu}_e$ /cm² sec) and takes cognizance of the distinctive signature of the reaction—a positron followed by the slowing down and capture of two neutrons, to help reduce the background to manageable proportions. Unlike the previous at-

[†] Supported in part by the U. S. Atomic Energy Commission.

* Now Assistant Commissioner, South Carolina Commission on Higher Education, Columbia, S. C. 29201.

¹ F. A. Nezrick and F. Reines, Phys. Rev. **142**, 852 (1966).

² F. Reines and C. L. Cowan, Phys. Rev. **107**, 1609 (1957).

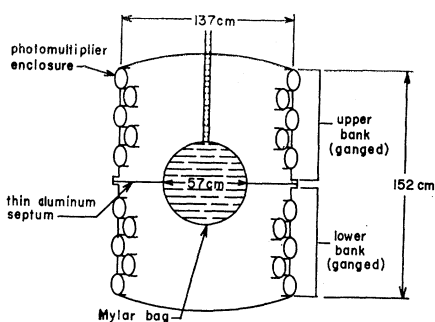


FIG. 1. Sketch of the 2240-liter scintillator tank. 132 photomultiplier tubes are mounted in steel cylinders welded to the tank wall. They view the liquid through clear plastic windows. The transparent spherical 2-mil-thick Mylar bag (Ref. 20) contains 97 liters of deuterated decalin-based scintillator with 2.6 g/liter of Gd in the form of gadolinium octoate. The scintillator in the outer region was essentially mineral oil, CH_2 , $\rho = 0.872 \text{ g/cm}^3$.

tempt, the deuterons were incorporated directly into the liquid scintillator solvent,³ deuteron-substituted decalin ($\text{C}_{10}\text{H}_8\text{D}_{10}$), $\rho = 0.957 \text{ g/cm}^3$, so that it became possible to obtain a measure of the spectrum of the short-range product positron. The target deuterons were located well inside a large scintillation detector which provided total absorption of the γ rays produced by annihilation of the positron and by capture of the neutrons. The detector had the further advantage that it shielded the inner target volume, containing the neutron-capturing Gd, from neutrons produced external to the detector by the reactor and by the capture of cosmic-ray muons.

The detector was operated in several configurations to establish the relationship between the signal and the antineutrino flux from the reactor. We demonstrated that the time-correlated signal disappeared when the deuterons were removed, that the signal disappeared when the reactor was turned off (Table II), and that the

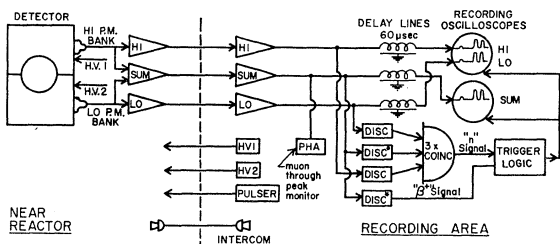


FIG. 2. Block diagram of electronics. Discriminators marked by an asterisk were upper and lower level, others were lower level only. Trigger logic required an e^+ signal followed within $60 \mu\text{sec}$ by two n signals. In addition to the features shown in this simplified diagram were scalars which recorded the various rates of interest, e.g., e^+ -like pulses, neutronlike pulses, and delayed coincidences with one or two neutrons. Also incorporated were such features as an automatic count stop, 10-kHz oscillator for oscilloscope time base calibration, and correction for system deadtime during camera advance after each trigger.

³ Dr. Henry M. Grotta of the Battelle Memorial Institute prepared the target material by deuteration of naphthalene. The scintillators employed and the detector are described by T. L. Jenkins and F. Reines, IEEE Trans. Nucl. Sci. NS-11, 1 (1964).

capture-time relationship was characteristic of neutrons in our scintillator.

EXPERIMENTAL ARRANGEMENT

The detector consisted of 2.24×10^3 liters of a scintillator based on mineral oil, surrounding 97 liters of the target volume of scintillator containing deuterons,³ all of which was viewed by 132 5-in. photomultiplier tubes Fig. 1. In order to reduce backgrounds due to chance coincidences from events which occur outside the target region, a light divider or septum was located around the equator of the bag between the upper and lower halves of the detector. In the case of the neutron capture pulses, a coincidence was required between the photomultiplier tubes located above (HI) and below (LO) the septum. This requirement does not drastically reduce the response to events which occur in the centrally placed bag because these events can be seen by both banks of photomultiplier tubes. However, because of the geometry, the background which originates primarily in regions nearest the tank wall is less well seen on the side of the light divider opposite its occurrence.

The response of the liquid scintillators to a weak Y^{88} source inside and outside the target bag were roughly matched. The ratio of responses inside to outside, typically 0.82, varied between 0.72 and 0.91 throughout the experiment. Thus, as a scintillator, the entire tank was reasonably homogeneous while only the central spherical region contained the gadolinium and the target deuterons. We employed the coincidence requirement between HI and LO photomultiplier tubes for the neutron pulses only, so as not to distort the first pulse spectrum. This reduced the background by a factor of 3 while reducing the neutron detection efficiency by approximately a factor of 2.

The electronics is shown as a block diagram in Fig. 2. When a delayed coincidence occurred in which the first, or positronlike, pulse in the energy range 1.75–6 MeV was followed within $60 \mu\text{sec}$ by two neutronlike pulses in the energy range $>1.5 \text{ MeV}$ in the upper and lower banks and totalling 5.5–10.0 MeV, the oscilloscopes were triggered. The upper and lower pulses, as well as the sum pulses which had been stored on the delay lines, were photographed. Since this mode of operation was sensitive to $d(\bar{\nu}_e, e^+)2n$, it was called the d mode. It was also found useful for calibration purposes to operate the equipment so as to be sensitive to the reaction $p(\bar{\nu}_e, e^+)n$ or the p mode. This was accomplished by requiring only one neutronlike pulse instead of two to trigger the oscilloscopes.⁴

The detector was enclosed in a massive lead shield to reduce the background due to reactor-associated γ rays.

Sample oscilloscope traces are shown in Fig. 3, where the information from the two banks of photomultiplier tubes is displayed for: a deuteronlike event [Figs. 3(a)

⁴ In this mode the first pulse discriminator was set at 2.25 MeV rather than 1.75 MeV.

TABLE I. Average count rates.

Configuration	Positron gate (min ⁻¹)	Neutron gate (min ⁻¹)	Delayed-coincidence triggers ^a (60- μ sec gate)		Calculated accidentals (60- μ sec gate)	
			p	d	p	d
A Deuteron bag (reactor on)	50 000	160	9.0	0.03	8	0.003
B Deuteron bag (reactor off)	43 000	64	2.8	0.03	2.5	0.0003
D No bag ^b (reactor on)	45 000	272	13	0.03	12	0.007
E No bag (reactor off)	35 000	117	6	0.04	4.1	0.001

^a Note the great excess of delayed coincidence triggers of the d type over the calculated accidental rate. These are due to the multiple pulse events such as that illustrated in Fig. 3(e) and are seen to be independent of reactor and the presence of deuterons in the target.

^b Bag volume occupied by CH₂ based scintillator without Gd.

and 3(b)], a protonlike event [Figs. 3(c) and 3(d)], and a noise or highly multiple delayed-coincidence burst [Fig. 3(e)]. Since noise bursts are shown (Table I) to be independent of the reactor and the presence of target deuterons, we will not discuss them further here.

OPERATION OF EQUIPMENT

The energy calibration of the scintillator was accomplished by immersing in it a weak Y⁸⁸ source, sealed in a thin-walled aluminum capsule. The resulting pulse-height spectrum showed a single peak corresponding to a total absorption of the γ rays emitted by the source (2.76 MeV). The full width of the peak at half-maximum was typically 20–25%. The gain of the system was measured at intervals of several weeks using this source, and was checked two times each day by the “through-peak” monitor which measured the characteristic response of the detector to cosmic-ray muons. The system

was found to be quite stable, varying less than $\pm 10\%$ in gain over periods of two to three months, provided the scintillator was not disturbed.⁵ Before and after every run calibration pulses for both pulse amplitude and time base were fed to the preamplifiers. Runs were made in the d and p modes with reactor on and off. A check was made of the relationship of noise events by running without the target bag. Table I lists the count rates typical of these operating modes.

DATA REDUCTION AND ANALYSIS

The film records obtained by photographing the HI-LO and SUM oscilloscopes were scanned, and the pulse amplitudes and relative times were recorded for each event. In the scanning procedure, all events exhibiting more than three pulses above the lower limit (1.75 MeV) of the amplitude for an e^+ -channel pulse within 60 μ sec after the first pulse were rejected. This

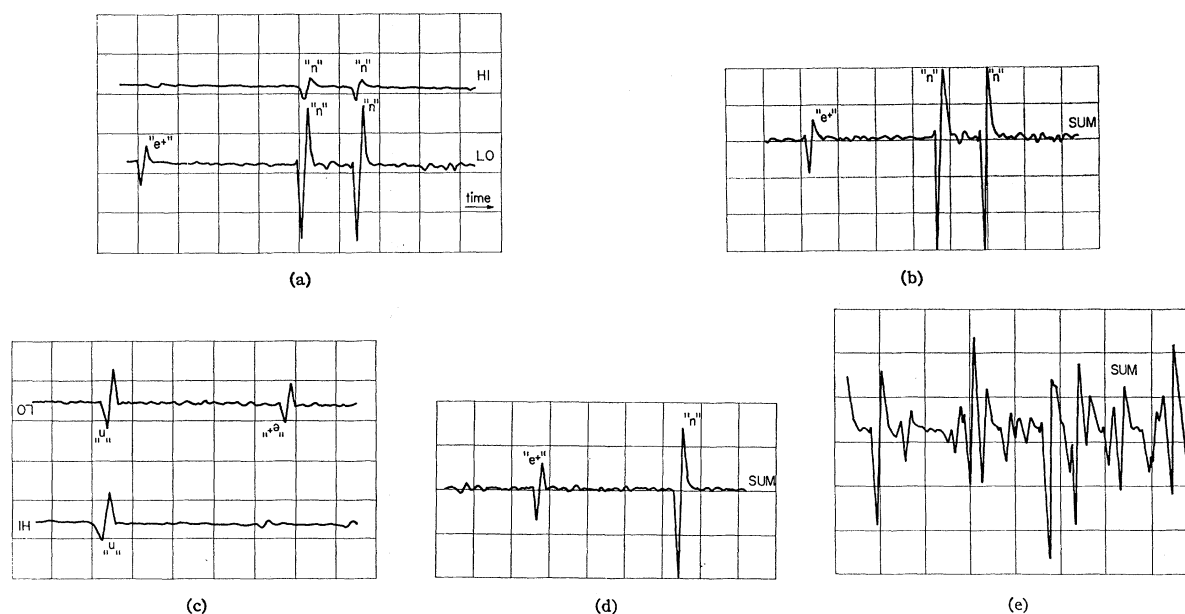


FIG. 3. (a) Deuteronlike event HI-LO scope (sweep length was 60 μ sec); (b) deuteronlike event SUM scope; (c) protonlike event HI-LO scope; (d) protonlike event SUM scope; and (e) noise event SUM scope.

⁵ A loss of $\sim 10\%$ in pulse height occurred when the deuterated scintillator was transferred from the bag to a container and back. The scintillation response of the liquid between transfers was constant within $\pm 3\%$.

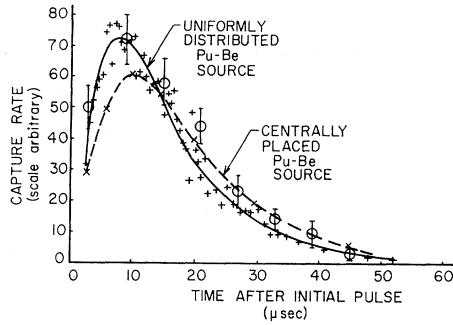


FIG. 4. Capture-time distributions for Pu-Be source centrally placed \times and uniformly distributed $+$. Also shown are results of Monte Carlo calculation Φ made assuming 1-keV initial neutron energy and infinite homogeneous medium.

eliminated a large class of multiple pulses which were observed to trigger the system by accidentally satisfying the coincidence requirements. In addition, acceptance was contingent on the SUM film showing the first or e^+ pulse with energy ≥ 1.75 MeV, and ≤ 6.0 MeV; both the second and third or neutron pulses with energy ≥ 5.5 MeV, and ≤ 10.0 MeV; and the time from the e^+ pulse to second neutron capture $\leq 60 \mu\text{sec}$. The HI-LO film was checked against the SUM record, and the further criterion that HI and LO traces have an energy > 1.5 MeV was applied.

NEUTRON CAPTURE VERSUS TIME

Since the identifying characteristic of the signal was the time correlation between the e^+ and neutron pulses, it was necessary to determine the capture versus time curve for a fast neutron introduced into the system. This was done by combining a series of curves taken at a series of radial positions with a Pu-Be source. The resulting distribution was taken to be representative of neutrons produced in the deuteron reaction. It is recognized that the spectrum expected from the deuteron reaction differs from that of the source, but the bag radius is sufficiently large [~ 1.5 m.f.p. (mean free path) for a 5-MeV and ~ 4 m.f.p. for a 1-MeV neutron] so that the effect of leakage on the capture-time distribution should be small. In these source measurement, the data were taken with the system operated in the \hat{p} mode except that the e^+ -channel gates were set to accept the 4.4-MeV prompt γ ray from the excited carbon produced in the reaction $\text{Be}^9(\alpha, n)\text{C}^{12*}$. The subsequent neutron capture was counted in the n channel. The results are shown in Fig. 4, which also includes the time distribution observed for a centrally placed source and the capture rates given by a Monte Carlo calculation in an infinite medium from an initial energy of 1 keV.

The effect of using the two drastically different capture-time curves in a maximum-likelihood fit described in the next section gives the results for the d -

mode, d -bag correlated rate:

$$0.119 \pm 0.025/h \text{ (distributed source),}$$

$$0.141 \pm 0.028/h \text{ (central source).}$$

This shows the insensitivity of the results to the precise form of the curve. The rate associated with the distributed source is chosen as representing the actual situation.

MAXIMUM-LIKELIHOOD CALCULATION OF TIME-CORRELATED RATES

We have used the high degree of time correlation expected in our experiment to distinguish the $d(\bar{\nu}_e, e^+)2n$ signal from uninteresting random backgrounds. A maximum-likelihood calculation was performed with filmed oscilloscope data consisting of the amplitudes of the e^+ channel, and the times to the first and second n -channel pulses t_1 and t_2 .

If the neutron-capture-time distribution is $g(t)$, then the differential probability distribution of t_1 and t_2 is

$$d^2N_S/dt_1dt_2 = g(t_1)g(t_2), \quad t_1 \leq t_2 \quad (2)$$

for the events arising from reaction (1). Events from random coincidences will have a distribution in t_1 and t_2 given by

$$d^2N_B/dt_1dt_2 = \tau^{-2}e^{-t_1/\tau}e^{-t_2/\tau}, \quad t_1 \leq t_2 \quad (3)$$

where τ is the mean time between n -channel pulses. τ was typically in the range 0.1–1 sec, and so the random coincidence background was essentially constant over the 60- μsec range of interest of t_1 and t_2 . The maximum-likelihood calculation then consisted of maximizing the function⁶

$$W(S, B) = \sum_i \ln[Sg(t_{1i})g(t_{2i}) + B] - \int_{t_1=t_{1ag}}^{t_{1max}} \int_{t_2=t_{1ag}+t_1}^{t_{2max}} [Sg(t_1)g(t_2) + B] dt_1 dt_2 \quad (4)$$

with respect to the signal S and the background rate B . t_{1ag} is the minimum time between pulses which can be clearly distinguished on the oscilloscope screen. This expression for $W(S, B)$ can be rewritten as

$$W(S, B) = \sum_i \ln[Sg(t_{1i})g(t_{2i}) + B] - S \times I - B \times A, \quad (5)$$

where $g(t)$ is the single neutron-capture-time distribution normalized so that

$$\int_{t_1=0}^{\infty} \int_{t_2=0}^{\infty} g(t_1)g(t_2) dt_1 dt_2 = 1, \quad (6)$$

⁶ This formula is an application of the extended maximum-likelihood method. See, e.g., J. Orear, University of California Lawrence Radiation Laboratory Report No. UCRL-8417, 1958 (unpublished).

TABLE II. Summary of maximum-likelihood results. *A*, *G*, *C*, and *F* have Gd in the target bag; *S* is the time-correlated signal; *B* is the random background.

Run configuration and mode	Integrated flux ($\bar{\nu}_e/\text{cm}^2$)	Run length (h)	Maximum likelihood (counts)	Rate (h^{-1})
<i>A</i> { <i>d</i> mode <i>d</i> bag	1.08×10^{20}	1079.5	$S = 129 \pm 27$ $B = (0.121 \pm 0.016)/\mu\text{sec}^2$	0.119 ± 0.025 0.403 ± 0.053^a (60- μsec gate)
<i>G</i> { <i>d</i> mode <i>d</i> bag	0	102.2	$S = 0 \pm 1$	0 ± 0.01
<i>C</i> ^b { <i>d</i> mode <i>p</i> bag	1.97×10^{19}	198.1	$S = 1.3 \pm 7.2$ $B = 0.0220 \pm 0.0066$	0.007 ± 0.036 0.399 ± 0.120
<i>D</i> { <i>d</i> mode no bag	5.49×10^{19}	571.6	$S = 3.2 \pm 5.3$ $B = 0.015 \pm 0.004$	0.0056 ± 0.0093 0.095 ± 0.025
<i>E</i> { <i>d</i> mode no bag	0	53.9	$S = 1 \pm 1$	0.02 ± 0.02
<i>F</i> ^c { <i>p</i> mode <i>d</i> bag	4.47×10^{18}	42.6	$S_p = 535 \pm 87$	12.6 ± 2.0

^a To obtain the random background rate from the listed figures, multiply *B* by the square of the delayed-coincidence-gate length in microseconds and divide by the run length in hours, e.g., $(0.121 \pm 0.016) \times (60)^2 / 1079.5 = 0.403 \pm 0.053$.

^b The time correlation between pulses was taken here to be that for the deuterated scintillator. Since the actual capture-time curve is more peaked towards shorter times, this assumption should accentuate the correlated signal, if any.

^c The signal here is for the reaction $\bar{\nu}_e e^+ n$. As described in the section below on the determination of ϵ_d , protons external to the bag contribute to the observed reaction rate. Neutrons produced in such external regions necessarily take more time, on the average, to diffuse to the bag and be captured by the Gd there. The time correlation associated with the centrally placed neutron source (Fig. 4) is, perhaps fortuitously, reasonably representative of this situation, and hence was used in calculating the reactor-associated signal.

and *I* is the double integral over the visible region

$$I = \int_{t_1=t_{lag}}^{t_{max}} \int_{t_2=t_{lag}+t_1}^{t_{max}} g(t_1)g(t_2)dt_1dt_2. \quad (7)$$

It is to be noted that *S* is the total number of signal events, visible plus invisible, and *B* is the similar total of background events, but per μsec^2 . In this experiment the summation over *i* extends over all the events for which the *n*-channel pulse delay times (t_{1i} and t_{2i}) lay within the limits $t_{1i} \geq t_{lag}$, $t_{2i} - t_{1i} \geq t_{lag}$, where $t_{lag} = 3.0 \mu\text{sec}$ and $t_{2i} \leq 60 \mu\text{sec}$. *W*(*S*,*B*) was maximized relative to *S* and *B* by a simple search procedure on the Case Univac 1107 computer. The results of these calculations are given in Table II. Errors given are statistical only and were calculated from the derivatives of the likelihood function at its maximum, i.e., at

$$\partial W / \partial \alpha_j = 0, \quad (8)$$

where $\alpha_1 = S$, $\alpha_2 = B$, and the errors in *S* and *B* are obtained from the error matrix.⁶

EFFICIENCY ϵ_d

Our interest is in determining the efficiency ϵ_d for detecting the reaction $d(\bar{\nu}_e e^+)2n$. This requires a knowledge of the efficiencies for positron and neutron detection, ϵ_{de^+} and ϵ_{dn} . The quantity ϵ_{dn} is determined by relating it to the detection efficiency for neutrons produced in the reaction $p(\bar{\nu}_e e^+)n$ observed with the same detector. Here ϵ_{de^+} is obtained from a consideration of the positron and neutron spectra predicted for $d(\bar{\nu}_e e^+)2n$. The ratio $\epsilon_{dn}/\epsilon_{pn}$ is a function only of the difference in the associated neutron spectra and the location of the reaction.

For the proton reaction,

$$\begin{aligned} \epsilon_{pn} &= R_p / n_p \sigma_p f \epsilon_{pe} \\ &= 0.63 \pm 0.11, \end{aligned} \quad (9)$$

where (see Ref. 7)

$$\begin{aligned} R_p &= 535 \pm 87, \text{ proton signal,} \\ n_p &= 3.05 \times 10^{27} \text{ protons (in target bag),} \\ \sigma_p &= (1.07 \pm 0.07) \times 10^{-43} \text{ cm}^2/\text{fission } \bar{\nu}_e, \\ f &= 4.47 \times 10^{18} \bar{\nu}_e/\text{cm}^2, \\ \epsilon_{pe^+} &= 0.58, \text{ positron detection efficiency,} \\ \epsilon_{pn} &= \text{neutron detection efficiency.} \end{aligned}$$

For the deuteron reaction,

$$\epsilon_{dn} = \left(\frac{\epsilon_{dn}}{\epsilon_{pn}} \right) \epsilon_{pn} = (0.63 \pm 0.11) \frac{\epsilon_{dn}}{\epsilon_{pn}}. \quad (10)$$

In this calculation ϵ_{dn} refers to a source of $\bar{\nu}_e$ -induced reactions which produces neutrons within the deuterated scintillator. ϵ_{pn} , on the other hand, takes into account the contribution from target protons both inside and outside of the deuterated bag.⁸ Here, the neutrons from the proton reaction are reasonably considered to be thermal,⁹ those from the deuteron reaction $\sim 0.25 \text{ MeV}$. A Monte Carlo calculation was made to determine the

⁷ ϵ_{pe^+} is the fraction of the positron spectrum with KE between >1.75 and $<4.6 \text{ MeV}$. This can be determined from the dashed curve in Fig. 11 of Ref. 1.

⁸ The apparent detection efficiency for the proton reaction is increased by virtue of the neutrons which are born outside the bag but diffuse and are captured by Gd in the bag.

⁹ In considering the leakage of neutrons in the several kilovolt range into and out of the bag, a plane approximation is excellent. Accordingly, the result is independent of initial neutron energy for the proton reaction.

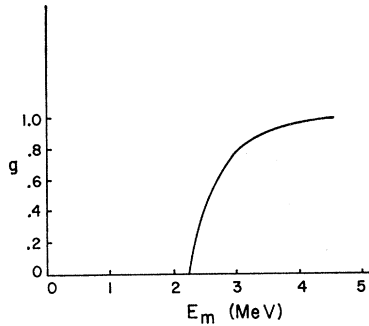


FIG. 5. Probability g of a first pulse to exceed the 2.25-MeV threshold versus E_m , the maximum energy available ($E_m = E_{\bar{\nu}_e} - 2.98$ MeV).

spatial distribution for the thermalized neutrons from the deuteron reaction starting from a uniform distribution throughout the deuterated target. The fraction thermalized in the bag was insensitive to the initial energy, remaining in the range 0.74 ± 0.06 for an energy range 0.01–1 MeV.

At this point an additional Monte Carlo calculation could have been performed to determine the probabilities of capture by the Gd in the deuterated scintillator in our 60- μ sec time gate for the proton and deuteron produced neutrons. However, this seemed too elaborate and the captures were estimated by means of time-independent diffusion theory. The trick here was to vary the capture cross section in the region external to the bag. In this way, the capture ratio $\epsilon_{pn}/\epsilon_{dn}$ was found to be relatively insensitive to the capture time in the external region, varying from 1.47 for 30- μ sec capture time to 1.65 for 90 μ sec.¹⁰ Since the time gate for acceptance of delayed coincidences was 60 μ sec, the value $\epsilon_{pn}/\epsilon_{dn} = 1.57$ calculated for this capture time was used in determining ϵ_{dn} . The final result is $\epsilon_{dn} = 0.40 \pm 0.07$.

An attempt was made to determine the neutron detection efficiency more directly by averaging the response to a Pu-Be source placed in various positions within the bag. The result was in agreement with the number quoted above, but the uncertainties were difficult to estimate.

The positron detection efficiency ϵ_{de^+} is somewhat complicated to determine for the deuteron reaction because of the three-particle final state which allows the positron a wide range of energies for each incident $\bar{\nu}_e$ energy. In determining the fraction of the first pulses seen with a given discriminator setting, it is therefore necessary to take into account the energy partition between the positron and neutrons and the relative

¹⁰ The diffusion-theory calculation showed that the probability of capture by the Gd for thermal neutrons varied from 0.97 for 10 μ sec to 0.98 for 90 μ sec when the neutrons were initially distributed uniformly throughout the bag. This result indicates the essential independence of the fraction of thermal neutrons captured in the bag with respect to the initial distribution of thermal neutrons in the bag.

efficiency with which neutrons produce scintillation light via recoil protons.¹¹

The energy partition has been calculated on a phase space basis for a similar situation.¹²

Figure 5 shows the probability g of a first-pulse energy exceeding the chosen threshold energy of 2.25 MeV plotted against E_m , the maximum energy available ($E_m = E_{\bar{\nu}_e} - 4.0 + 1.02$ MeV).

The calculation of positron detection efficiency ϵ_{de^+} is completed by determining the fraction of the positron spectrum above the threshold 2.25 MeV having folded in the cross section $\sigma_d(E_{\bar{\nu}_e})$,¹³ the fission $\bar{\nu}_e$ spectrum $n(E_{\bar{\nu}_e})$,¹⁴ and the factor g .

$$\epsilon_{de^+} = \int_{2.25}^{\infty} n \sigma_d g dE_{e^+} / \int_{2.25}^{\infty} n \sigma_d dE_{e^+} = 0.63. \quad (11)$$

Combining ϵ_{dn} and ϵ_{de^+} , we obtain

$$\epsilon_d = \epsilon_{de^+} \epsilon_{dn}^2 = 0.10 \pm 0.034. \quad (12)$$

CROSS SECTION σ_d

We are now in a position to evaluate the experimentally determined cross section $\bar{\sigma}_d$ for the reaction $d(\bar{\nu}_e, e^+)2n$ averaged over the fission $\bar{\nu}_e$ spectrum.

$$\begin{aligned} \bar{\sigma}_d &= R_d / n_d f \epsilon_d \\ &= (2.9 \pm 1.5) \times 10^{-45} \text{ cm}^2 / \text{fission } \bar{\nu}_e, \end{aligned}$$

where

$$\begin{aligned} R_d &= 121 \pm 47, \text{ deuteron signal,} \\ n_d &= 3.82 \times 10^{27} \text{ deuterons (in target bag),} \\ f &= 1.08 \times 10^{20} \bar{\nu}_e / \text{cm}^2, \\ \epsilon_d &= 0.10 \pm 0.034. \end{aligned} \quad (13)$$

The small adjustment described in Ref. 15 raises this

¹¹ The apparent energy E_0 of a recoil proton of energy E_p in the ≤ 1 -MeV range is $E_0 = 0.26 E_p$. See J. H. Munsee and F. Reines, Phys. Rev. **177**, 2002 (1969).

¹² The calculation performed in this reference was for the reaction $\bar{\nu}_e + d \rightarrow p + n + \bar{\nu}_e$. See Appendix I of Ref. 11. In order to apply it to the present case the energy of the outgoing $\bar{\nu}_e$ is replaced by the energy of the product positron. A more precise treatment by A. McCone, Jr. (private communication) in which various scattering lengths are considered for the final-state interaction gives the same result within a few percent.

¹³ J. Weneser, Phys. Rev. **105**, 1335 (1957). The cross section given in this reference should be multiplied by a factor of 2 because parity is not conserved.

¹⁴ The earliest calculation of the expected cross section was made by C. O. Muelhause and S. Oleksa, Phys. Rev. **105**, 1332 (1957), who measured the equilibrium beta spectrum from fission, deduced the antineutrino spectrum, and applied the theory of Weneser (Ref. 13). Their result, adjusted for the parity factor, is 4×10^{-45} cm². A more precise measurement of the fission beta spectrum was made by R. E. Carter, F. Reines, J. J. Wagner, and M. E. Wyman, Phys. Rev. **113**, 280 (1959).

¹⁵ Since it may be of importance to future measurements of $\bar{\sigma}_d$, we note that a small correction to this cross section is required because of the contribution to the proton mode of deuteron events in which only one neutron was detected. Simple combinatorial analysis shows that each deuteron reaction has a probability P_1 of producing only one detected neutron, $P_1 = 2\epsilon_{dn}(1 - \epsilon_{dn})$. If we take into account \bar{P}_1 , the relative number of protons and deuterons, and the ratio $\bar{\sigma}_p/\bar{\sigma}_d$, the resultant efficiency for detection of the proton reaction should be lowered by approximately 2%. This implies an increase in the deduced value of $\bar{\sigma}_d$ of approximately 4%.

value to

$$\bar{\sigma}_d = (3.0 \pm 1.5) \times 10^{-45} \text{ cm}^2/\text{fission } \bar{\nu}_e.$$

This cross section is to be compared with the theoretically expected value (see the Appendix). Using the work of Weneser for $\sigma_d(E_{\bar{\nu}_e})$ and the spectrum $n(E_{\bar{\nu}_e})$ of Carter *et al.*, the value $\bar{\sigma}_d = 1.7 \times 10^{-45} \text{ cm}^2/\text{fission } \bar{\nu}_e$ is obtained. A better measured fission beta spectrum due to Wyman and Kutcher¹⁶ leads to a more accurate $\bar{\nu}_e$ spectrum and a predicted $\bar{\sigma}_d = (2.2 \pm 0.4) \times 10^{-45} \text{ cm}^2/\text{fission } \bar{\nu}_e$. The error in $\bar{\sigma}_d$ reflects primarily the uncertainty in the Gamow-Teller β coupling constant as quoted by Winther and Kofoed-Hansen.¹⁷

A thorough study of fission chains by Avignone *et al.*¹⁸ leads to a $\bar{\nu}_e$ spectrum from which a value of $\bar{\sigma}_d = (2.4 \pm 0.4) \times 10^{-45} \text{ cm}^2/\text{fission } \bar{\nu}_e$ is deduced.

We find no disagreement between theory and experiment but the errors are too large to make a detailed comparison.

Argument That d -Mode Signal Is Due to $d(\bar{\nu}_e, e^+)2n$ Reaction (Table II)

A comparison of A and G shows a time-correlated reactor-associated signal S . A and C indicate that the signal is associated with the presence of target deuterons. Runs D and E are consistent with the absence of a signal when deuterons and Gd capturer are absent. Further identification of the reaction is provided by the time correlation of the data shown in Fig. 6 which is consistent with that expected for the known capture-time distribution of neutrons in the target.

A maximum-likelihood analysis of the data obtained in configuration A yielded a crude spectrum of first pulses, i.e., those due to the positron slowing down and annihilating and the neutron slowing down. This spectrum as well as the first-pulse spectrum due to accidental delayed coincidences is shown in Table III.

Argument That p -Mode Signal Is Due to $p(\bar{\nu}_e, e^+)n$

Independent runs not shown in Table II indicate the presence of a time-correlated reactor-associated signal S . These runs were consistent with the absence of a signal when the reactor was off. The problem here is to be convinced that the reactor-associated time-correlated signal listed in Table II was not due to neutrons making a recoil-proton pulse and then being captured in the centrally located Gd.

¹⁶ M. E. Wyman and J. Kutcher (private communication); J. W. Kutcher, Ph.D. thesis, University of Illinois, 1966 (unpublished).

¹⁷ A. Winther and O. Kofoed-Hansen, Kgl. Danske Videnskab. Selskab, Mat.-Fys. Medd. **26**, No. 6 (1951); Phys. Rev. **82**, 96 (1951). These authors give $C_{GT}^2/C_F^2 = 1.28 \pm 0.04$, and $g_p^2 = (0.50 \pm 0.06) \times 10^{-22}$. Since $g_d^2/g_p^2 = 3C_{GT}^2/(3C_{GT}^2 + C_F^2)$, one obtains $g_d^2 = (0.40 \pm 0.05) \times 10^{-22}$. E. J. Konopinski and L. M. Langer, in *Annual Reviews of Nuclear Science* (Annual Reviews, Inc., Stanford, Calif., 1953), Vol. 3, p. 261, quote a larger uncertainty, $\sim 30\%$ in g_d^2 .

¹⁸ F. T. Avignone III, S. M. Blankenship, and C. W. Darden III, Phys. Rev. **170**, 931 (1968).

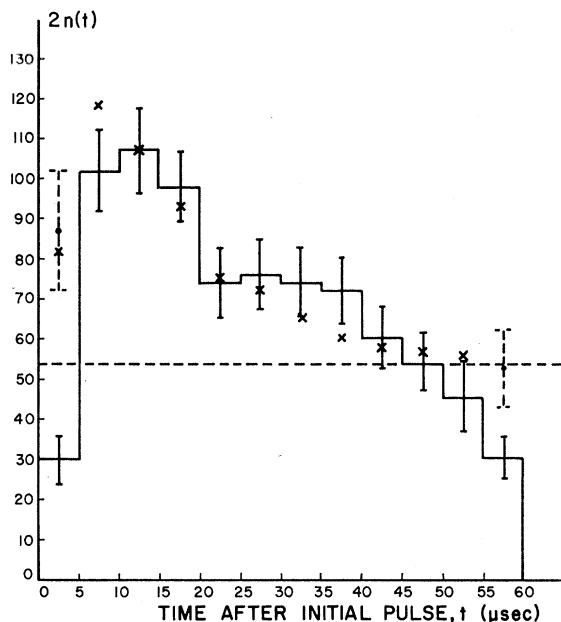


Fig. 6. Measured capture-time distribution run A (d mode, d bag). Notes: (1) 0–5 and 55–60 μsec values adjusted to take account of loss of pulses due to 3- μsec resolving time (t_{142}) of oscilloscope record. 0–5 μsec scaled up to $\frac{5}{2}$, 55–60 μsec scaled up by $\frac{5}{2} + \frac{1}{2} \times \frac{5}{2} = 1.75$. (2) Crude fit made to measured neutron capture-time curve. Points denoted by \times .

This possibility is ruled out by the shielding which the outer scintillation liquid (≥ 37 cm thick, $\rho = 0.9 \text{ g/cm}^3$) provides to the neutron-capturing target. An earlier experiment¹⁹ showed that a reactor-associated signal obtained with an unshielded target region was not affected by the addition of such a shielding thickness although the response to an Am-Be neutron source was reduced by a factor of 15.

IMPROVEMENTS

The experiment could be improved in several ways: Sharpen the time resolution so as to avoid the losses due to the overlap of pulses; reduce the accidental background by decreasing the neutron-capture time and hence the 60- μsec time gate; increase counting times so as to reduce statistical errors. If all these steps were taken, then a more thoroughgoing series of calculations of positron and neutron spectra and associated neutron

TABLE III. Spectrum of first pulses from reaction $d(\bar{\nu}_e, e^+)2n$ and the accidental background spectrum.

E (MeV)	Signal (MeV ⁻¹)	Accidental background (60- μsec time gate)
2.6	87 ± 27	332 ± 57
3.5	35 ± 15	143 ± 33
4.8	18 ± 7	32 ± 12

¹⁹ F. Reines and C. L. Cowan, Phys. Rev. **113**, 273 (1959).

slowing down and diffusion would be warranted as a basis for more precise interpretation of the data.

ACKNOWLEDGMENTS

We wish to thank Dr. J. Weneser and Dr. C. Werntz for theoretical discussion and calculations of the reaction, and Mrs. R. Alexander for help in preparing and running the necessary computer programs. Dr. J. Munsee performed some of the diffusion-theory calculations used to compare the efficiencies in the proton and deuteron modes. B. Shoffner designed and built special coincidence circuits, and A. A. Hruschka was most helpful in the mechanical design, construction, and installation of the detector. We are grateful to our hosts, the E. I. Dupont de Nemours and Company, Inc., for their hospitality at the Savannah River Plant.

APPENDIX: PREDICTED VALUE OF $\bar{\sigma}_d$ FOR FISSION SPECTRUM $\bar{\nu}_d$

$$\bar{\sigma}_d = \frac{\int_{4.0}^{\infty} n(E_{\bar{\nu}_e})\sigma_d(E_{\bar{\nu}_e})dE_{\bar{\nu}_e}}{\int_0^{\infty} n(E_{\bar{\nu}_e})dE_{\bar{\nu}_e}}$$

$$\int_0^{\infty} n(E_{\bar{\nu}_e})dE_{\bar{\nu}_e} = 6.1\bar{\nu}_e/\text{fission} \quad (A1)$$

TABLE IV. $\bar{\nu}_e$ spectrum and cross section for $d(\bar{\nu}_e, e^+)2n$.

$E_{\bar{\nu}_e}$ (MeV)	$\sigma_d \times 10^{44}$ (cm ²)	n ($\bar{\nu}_e$ /fission MeV)	$n\sigma_d \times 10^{44}$
4.0	0	0.28	0
4.5	0.73	0.16	0.18
5	2.96	0.10	0.30
5.5	6.84	0.06	0.41
6	12.3	0.038	0.47
6.5	19.4	0.023	0.45
7	28.8	0.010	0.29
7.5	40.0	0.006	0.24
8	53.2	0.0038	0.20
8.5	68.0	0.0012	0.08
9	85.0	0.0005	0.05
10	125.0	0.00005	0

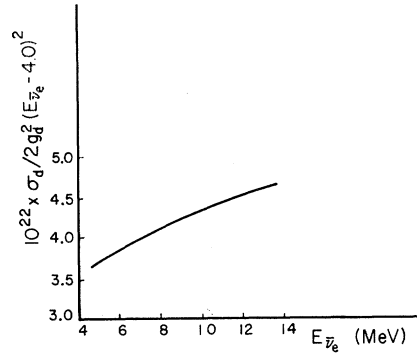


FIG. 7. Energy dependence of cross section for reaction $d(\bar{\nu}_e, e^+)2n$ after Weneser (Ref. 13). $2g_d^2 \times 10^{-22} = 8 \times 10^{-46}$ cm²/MeV².

where $n(E_{\bar{\nu}_e})$ is the fission $\bar{\nu}_e$ spectrum, and $\sigma_d(E_{\bar{\nu}_e})$ is the theoretical cross section for $\bar{\nu}_e$ of energy $E_{\bar{\nu}_e}$.

From Weneser's paper we derive Fig. 7, which enables an interpolation for $\sigma_d(E_{\bar{\nu}_e})$ between the values which he calculated.

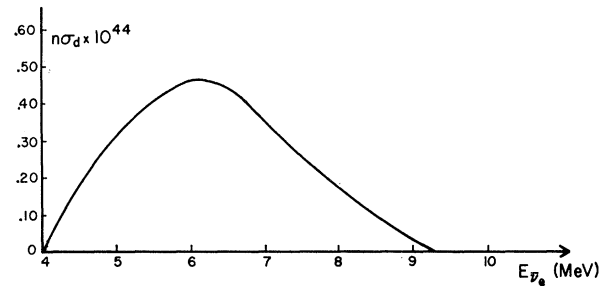


FIG. 8. Probability of reaction per fission versus antineutrino energy.

The neutrino spectrum $n(E_{\bar{\nu}_e})$ is derived from the work of Wyman and Kutcher¹⁶ by simply reading $E_{\bar{\nu}_e} = E_{\beta^-} + 0.51$ MeV. Table IV lists $\sigma_d(E_{\bar{\nu}_e})$, $n(E_{\bar{\nu}_e})$, and $n\sigma_d$ in the range 4-10 MeV. Figure 8 is a plot of $n\sigma_d$.